

# Enzyme–DNA Biocolloids for DNA Adduct and Reactive Metabolite Detection by Chromatography–Mass Spectrometry

Besnik Bajrami,<sup>†</sup> Eli G. Hvastkovs,<sup>†</sup> Gary C. Jensen,<sup>†</sup> John B. Schenkman,<sup>‡</sup> and James F. Rusling<sup>\*†‡</sup>

Department of Chemistry, University of Connecticut, Storrs, Connecticut 06269-3060, and Department of Cell Biology, University of Connecticut Health Center, Farmington, Connecticut 06032

Silica microbead bioreactors (0.5  $\mu\text{m}$  diameter) coated with DNA and enzymes were fabricated to measure reactive metabolite and DNA–adduct formation rates relevant to genotoxicity screening. Cytochrome (cyt) P450 2E1, cyt P450<sub>cam</sub>, and myoglobin (Mb) were incorporated into thin films with DNA using the electrostatic layer-by-layer (LbL) method. The utility of these biocolloids was demonstrated by oxidation of guaiacol, styrene, and (4-methylnitrosoamino)-1-(3-pyridyl)-1-butanone (NNK). Enzyme turnover rates for formation of reactive metabolites were monitored using gas chromatography/mass spectrometry (GC/MS) and liquid chromatography–mass spectrometry (LC–MS). Capillary LC–MS/MS was employed to determine DNA nucleobase adducts after catalyzing the reactive metabolite formation with DNA–enzyme biocolloids and then using neutral thermal hydrolysis on the biocolloids. Dramatic improvements in surface area to volume ratio over similar films on macroscopic surfaces opens new avenues for genotoxicity screening and enabled the first use of pure cyt P450 enzymes in enzyme–DNA films to produce DNA adducts. The method makes possible identification and formation rate measurements of major and minor DNA adducts as well as the metabolites themselves in <5 min of reaction time using relevant human liver enzymes.

Toxicity is often not identified sufficiently early in developing new pharmaceutical, agricultural, personal care, and dietary products. Roughly 30% of drug development failures result from toxicity issues, driving drug costs up significantly.<sup>1–4</sup> Conventional in vitro biological tests such as Ames, chromosome aberration, mouse lymphoma, and Comet assays provide qualitative answers to toxicity questions based on bulk DNA damage but do not give chemical structure or site-specific DNA damage information.<sup>5,6</sup> Animal testing may not relate to human exposure because of

metabolic and physiological differences between humans and animal models.<sup>2,4,7</sup> While all these toxicity tests are valuable, we believe that rapid, high-throughput toxicity screening methods for new chemicals that provide chemical structure information about reactive intermediates at early stages of commercial development are important goals to complement conventional microbiological and animal tests.

Bioactivation of xenobiotic molecules by metabolic enzymes often results in reactive metabolites that damage biomolecules, including DNA, in a major toxicity pathway.<sup>8–10</sup> An example is the metabolism of lipophilic compounds by liver cytochrome (cyt) P450 (or CYP) enzymes creating reactive electrophilic metabolites.<sup>4,11</sup> These electrophiles attack nucleophilic DNA sites, primarily guanines, potentially resulting in *genotoxicity*. Depending on the adduct site, additional metabolism, and DNA repair processes, covalent DNA adducts can lead to mutations, teratogenesis, and carcinogenesis.<sup>12–14</sup> Thus, nucleobase adducts are key biomarkers for predicting cancer risk in humans and for exposure to toxic chemicals, and sensitive liquid chromatography–mass spectrometry (LC–MS) methods have been developed for their in vivo detection.<sup>15–17</sup>

DNA damage can also be used as an endpoint in predicting the toxicity of new chemicals.<sup>18</sup> We have developed biosensors<sup>19</sup>

\* Corresponding author. E-mail: James.Rusling@uconn.edu.

<sup>†</sup> University of Connecticut, Storrs.

<sup>‡</sup> University of Connecticut Health Center.

(1) Rawlins, M. D. *Nat. Rev. Cancer* 2004, 3, 360–364.

(2) Caldwell, G. W.; Yan, L. *Curr. Opin. Drug Discovery Dev.* 2006, 9, 47–50.

(3) Nassar, A. E.; Kamel, A. M.; Clarimont, C. *Drug Discovery Today* 2004, 9, 1055–1064.

(4) Guengerich, F. P. *Am. Assoc. Pharm. Sci. J.* 2006, 8, E101–E111.

(5) Newton, R. K.; Aardema, M.; Aubrecht, J. *Environ. Health Perspect.* 2004, 112, 420–422.

(6) Kirkland, D.; Aardema, M.; Henderson, L.; Muller, L. *Mutat. Res.* 2005, 584, 1–256.

(7) Mayne, J. T.; Kum, W. W.; Kennedy, S. P. *Curr. Opin. Drug Discovery Dev.* 2006, 9, 75–83.

(8) Singer, B.; Grunberger, D. *Molecular Biology of Mutagens and Carcinogens*; Plenum Press: New York, 1983.

(9) Jacoby, W. B., Ed. *Enzymatic Basis of Detoxification*; Academic: New York, 1980; Vols. I and II.

(10) Friedberg, E. C. *Nature* 2003, 421, 436–440.

(11) (a) Schenkman, J. B.; Greim, H., Eds. *Cytochrome P450*; Springer-Verlag: Berlin, 1993. (b) Ortiz de Montellano, P. R., Ed. *Cytochrome P450*; Plenum: New York, 1995. (c) Singer, B.; Grundberger, D. *Molecular Biology of Mutagens and Carcinogens*; Plenum: New York, 1983.

(12) Scharer, O. D. *Angew. Chem., Int. Ed.* 2003, 42, 2946–2974.

(13) (a) Farmer, P. B. *Toxicol. Lett.* 2004, 149, 3–9. (b) Sharma, R. A.; Farmer, P. B. *Clin. Cancer Res.* 2004, 10, 4901–4912. (c) Baird, W. M.; Mahadeva, B. *Mutat. Res.* 2004, 547, 1–4.

(14) Hemminki, K.; Koskinen, M.; Rajaniemi, H.; Zhao, C. *Regul. Toxicol. Pharmacol.* 2002, 32, 264–275.

(15) Appuzzese, W. A.; Vouros, P. J. *Chromatogr., B* 1999, 794, 97–108.

(16) Vanhoutte, K.; Dongen, W.; Hoes, I.; Lemièrre, F.; Esmans, E. L.; Van Onckelen, H.; Van den Eckhout, E.; Soest, R. E. J.; Hudson, A. J. *Anal. Chem.* 1997, 69, 3161–3168.

(17) Gangl, E. T.; Turesky, R. J.; Vouros, P. *Anal. Chem.* 2001, 73, 2397–2404.

(18) Rusling, J. F.; Hvastkovs, E. G.; Schenkman, J. B. *Curr. Opin. Drug Discovery Dev.* 2007, 10, 67–73.

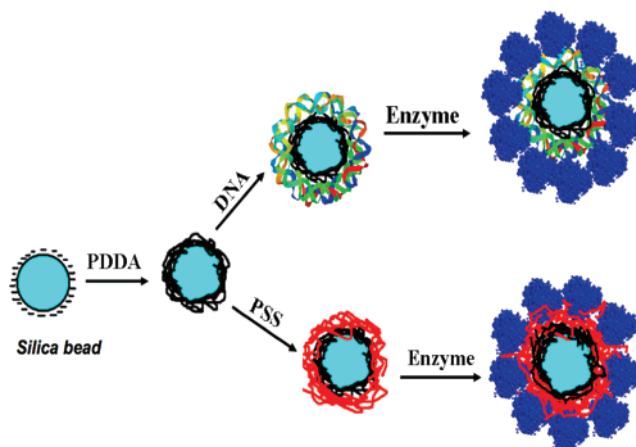
and arrays based on this principle for early toxicity screening featuring thin films of DNA and cyt P450 enzymes using voltammetric<sup>20</sup> and electrochemiluminescent (ECL) platforms.<sup>21</sup> The enzymes in these films metabolize drug or pollutant substrates to produce possible reactive metabolites that may form DNA adducts. High-throughput electrochemical and ECL arrays can provide simultaneous, rapid assessment of relative DNA damage rates from chemicals and metabolites from a range of enzymes.<sup>18,20,21</sup> While they provide relative rates of DNA damage, these arrays provide limited structural or formation rate information about specific nucleobase adducts. To obtain this information, damaged nucleobases can be isolated from the DNA and detected using LC-MS.<sup>22</sup>

We previously detected nucleobase adducts employing thin films of DNA and enzymes on high surface area carbon cloth.<sup>23</sup> However, carbon cloth does not have a well-defined surface area and requires significant amounts of enzyme, DNA, and polymer, along with significant solution volumes to fabricate films and obtain sufficient DNA adducts for analysis. For these reasons, immobilization of valuable cyt P450 enzymes for the evaluation of their metabolite-nucleobase adducts in thin films using LC-MS was not realized until now. Quite simply, purified cyt P450 enzymes are difficult to obtain in sufficient amounts to make usable enzyme-DNA films on carbon cloth.

To address these issues, we explored a biocolloid approach pioneered by Lvov, Caruso, and co-workers<sup>24</sup> who used alternate electrostatic layer-by-layer (LbL) adsorption<sup>25-28</sup> to form active enzyme films of glucose oxidase, horseradish peroxidase, and urease on spherical nanoparticles. The small size of the biocolloids offers increased active surface area and tiny solution volumes to conserve enzyme and also to obtain more product per unit time for subsequent determination of major and minor products.

In a recent short communication, we reported using cyt P450E1 films on microbeads to produce reactive metabolites of *N*-nitrosopyrrolidine.<sup>29</sup> We detected DNA damage using separate ECL arrays. Herein, we describe the preparation and characterization of more versatile biocolloids that feature coatings of DNA and metabolic enzymes (Scheme 1) aimed toward genotoxicity

### Scheme 1. Conceptual Illustration of DNA/Enzyme Film Formation on Silica Microbeads<sup>a</sup>



<sup>a</sup> Layer-by-layer electrostatic assembly is used to immobilize positively charged PDPA on the negative microbeads, followed by sequential adsorption of polyanion PSS or DNA and a positively charged enzyme layer (blue circles).

screening. Biocatalysts include cyt P450<sub>cam</sub>, cyt P450 2E1, and myoglobin (Mb). Cyt P450<sub>cam</sub> has been used as a model for human cyt P450s since it can be purified in higher yields than the human isoforms.<sup>20,21</sup> Mb is an easily obtainable model that behaves as an oxidoreductase or a peroxidase when activated by peroxide.<sup>30</sup> Cyt P450 2E1 is a human liver enzyme involved extensively in drug and xenobiotic metabolism,<sup>4</sup> including the metabolism of carcinogenic *N*-nitroso compounds.<sup>31</sup> Each of these enzymes was activated by small concentrations of hydrogen peroxide in the reverse of the well-known hydrogen peroxide shunt.<sup>19-21,23</sup> It is well-established that metabolite specificity is a property of the terminal oxidase, cyt P450, and that hydrogen peroxide or organic hydroperoxides activate cyt P450 to yield the same products<sup>32</sup> with possible deviations in product distribution.<sup>11b,33</sup> In cases examined in our laboratory to date,<sup>19-21,23,29,34,43</sup> we have not found that

(19) Zhou, L.; Yang, J.; Estavillo, C.; Stuart, J. D.; Schenkman, J. B.; Rusling, J. F. *J. Am. Chem. Soc.* **2003**, *125*, 1431-1436.  
 (20) Wang, B.; Jansson, I.; Schenkman, J. B.; Rusling, J. F. *Anal. Chem.* **2005**, *77*, 1361-1367.  
 (21) Hvastkovs, E. G.; So, M.; Krishnan, S.; Bajrami, B.; Tarun, M.; Jansson, I.; Schenkman, J. B.; Rusling, J. F. *Anal. Chem.* **2007**, *79*, 1897-1906.  
 (22) Tarun, M.; Rusling, J. F. *Crit. Rev. Eukaryotic Gene Expression* **2005**, *15*, 295-315.  
 (23) Tarun, M.; Bajrami, B.; Rusling, J. F. *Anal. Chem.* **2006**, *78*, 624-627.  
 (24) (a) Lvov, Y.; Caruso, F. *Anal. Chem.* **2001**, *73*, 4212-4217. (b) Shutava, T.; Zheng, Z.; John, V.; Lvov, Y. *Biomacromolecules* **2004**, *5*, 914-921. (c) Caruso, F.; Möhwald, H. *J. Am. Chem. Soc.* **1999**, *121*, 6039-6046. (d) Fang, M.; Grant, S. P.; McShane, M. J.; Sukhorukov, G. B.; Golub, V. O.; Lvov, M. Y. *Langmuir* **2002**, *18*, 6336-6344. (e) Caruso, F.; Schüler, C. *Langmuir* **2000**, *16*, 9595-9603. (f) Caruso, F.; Lichtenfeld, H.; Giersig, M.; Möhwald, H. *J. Am. Chem. Soc.* **1998**, *120*, 8523-8524.  
 (25) Lvov, Y. In *Protein Architecture: Interfacing Molecular Assemblies and Immobilization Biotechnology*; Lvov, Y., Möhwald, H., Eds.; Marcel Dekker: New York, 2000; pp 125-167.  
 (26) Lvov, Y. In *Handbook of Surfaces And Interfaces of Materials Vol. 3. Nanostructured Materials, Micelles and Colloids*; Nalwa, R. W., Ed.; Academic Press: San Diego, CA, 2001; pp 170-189.  
 (27) Ariga, K.; Hill, J. P.; Ji, Q. *Phys. Chem. Chem. Phys.* **2007**, *9*, 2319-2340.  
 (28) Zhang, X.; Chen, H.; Zhang, H. *Chem. Commun.* **2007**, 1395-1405.  
 (29) Krishnan, S.; Hvastkovs, E. G.; Bajrami, B.; Jansson, I.; Schenkman, J. B.; Rusling, J. F. *Chem. Commun.* **2007**, 1713-1715.

(30) (a) Guengerich, F. P. *Chem. Res. Toxicol.* **2001**, *14*, 611-650. (b) Cirino, P. C.; Arnold, F. H. *Angew. Chem., Int. Ed.* **2003**, *42*, 3299-3301. (c) Ortiz de Montellano, P. R.; Catalano, C. E. *J. Biol. Chem.* **1985**, *260*, 9265-9271.  
 (31) Hecht, S. S. *Chem. Res. Toxicol.* **1998**, *11*, 559-603.  
 (32) (a) Adams, C.; Adams, P. A. *J. Inorg. Biochem.* **1992**, *45*, 47-52. (b) Rahimtula, A. D.; O'Brien, P. J.; Seifried, H. E.; Jerina, D. M. *Eur. J. Biochem.* **1978**, *89*, 133-141. (c) Werringer, J.; Kawano, S.; Estabrook, R. W. In *Microsomes Drug Oxidations, and Chemical Carcinogenesis*; Coon, M. C., Estabrook, R. W., Gelboin, H. V., Eds.; Academic Press: New York, 1980; pp 403-406. (d) White, R. E.; Slinger, S. G.; Coon, M. W. *J. Biol. Chem.* **1980**, *255*, 11108-11111.  
 (33) (a) Bichara, N.; Ching, M. S.; Blake, C. L.; Ghabrial, H.; Smallwood, R. A. *Drug Metab. Dispos.* **1996**, *24*, 112-118. (b) Kupfer, R.; Liu, S. Y.; Allentoff, A. J.; Thompson, J. A. *Biochemistry* **2001**, *40*, 11490-11501.  
 (34) Estavillo, C.; Lu, Z.; Jansson, I.; Schenkman, J. B.; Rusling, J. F. *Biophys. Chem.* **2003**, *104*, 291-296.  
 (35) Nassar, A.-E. F.; Willis, W. S.; Rusling, J. F. *Anal. Chem.* **1995**, *67*, 2386-2392.  
 (36) Gillam, E. M. J.; Guo, Z. Y.; Guengerich, F. P. *Arch. Biochem. Biophys.* **1994**, *312*, 59-66.  
 (37) O'Keefe, D. H.; Ebel, R. E.; Petersen, J. A. *Methods Enzymol.* **1978**, *52*, 151-157.  
 (38) Omura, T.; Sato, R. *J. Biol. Chem.* **1964**, *239*, 2379-2385.  
 (39) Maehly, A.; Chance, B. *Methods Biochem. Anal.* **1954**, *1*, 357.  
 (40) Adam, W.; Lazarus, M.; Saha-Möller, C. R.; Weichold, O.; Hoch, U.; Häring, D.; Schreier, P. *Adv. Biochem. Eng. Biotechnol.* **1999**, *63*, 73-108.  
 (41) Doerge, D. R.; Divi, R. L.; Churchwell, M. I. *Anal. Biochem.* **1997**, *250*, 10-17.  
 (42) Gao, J.; Rusling, J. F.; Zhou, D. *J. Org. Chem.* **1996**, *61*, 5972-5977.

products formed via hydrogen peroxide activation differ in any way from those formed via the natural reductase cycle.

In this paper, we show for the first time that the higher enzyme activity and smaller reaction volumes afforded by DNA–enzyme biocolloids allow the use of pure human cyt P450 enzymes to generate and identify metabolite–nucleobase adducts using cyt P450–DNA films. This approach provides a facile, rapid, enzyme economic method to identify and quantify metabolites and adducted nucleobases alike using biologically relevant enzymes.

## EXPERIMENTAL SECTION

**Chemicals and Materials.** Double-stranded salmon testes (st) DNA (~2 K base pairs, 41.2% G/C) was from Sigma. Horse heart myoglobin (MW 17 400, 3 mg mL<sup>-1</sup>, 10 mM pH 5.5 ammonium acetate buffer) from Sigma was filtered through an Amicon YM30 membrane (MW 30 000 cutoff).<sup>35</sup> Polydiallyldimethylammonium chloride (PDDA, MW <200 000), polystyrene sulfonate (PSS, MW 70 000), styrene, styrene oxide, (4-methylnitrosoamino)-1-(3-pyridyl)-1-butanone (NNK), 4-hydroxy-1-(3-pyridyl)-butanone (HPB), and *o*-methoxyphenol (guaiacol) were from Sigma. Cyt P450 2E1 (CYP2E1; MW 52 000)<sup>36</sup> and cyt P450<sub>cam</sub> (CYP101; MW 46 500),<sup>37</sup> were expressed from DH5α *E. coli* containing the proper cDNA and isolated and purified according to the referenced procedures. The concentration of cyt P450 was assayed by the method of Omura and Sato.<sup>38</sup> Water was purified with a Hydro Nanopure system to a specific resistance of >16 MΩ·cm. All other chemicals were reagent grade. Hydrophilic silica microbeads were from Polyscience, Inc. (500 nm (±10%) diameter, approximately 10% solids,  $d = 1.96 \text{ g/cm}^3$ ) and were used after resuspension and proper vortex agitation to ensure solution homogeneity.

**Film Assembly on Microbeads.** A volume of 0.2 mL of stock dispersed microbeads in water (~2 × 10<sup>11</sup> beads) was added to PDDA (2 mg mL<sup>-1</sup>, 50 mM NaCl) in a total volume of 1.0 mL for 20 min to allow for steady-state adsorption.<sup>46</sup> This dispersion was then centrifuged for 4 min at 8000 rpm to remove microbeads from the PDDA solution, followed by three washings with pure water and 2 min of centrifugation at 8000 rpm. The microbeads were then resuspended in 1.0 mL of PSS solution (2.0 mg mL<sup>-1</sup>, 0.5 M NaCl) for 20 min, followed by the same centrifugation and washing steps. These microbeads were immersed in 0.5 mL of biocatalyst solution, i.e., Mb, cyt P450<sub>cam</sub> (both 100 μL, 0.57 mg mL<sup>-1</sup>, 10 mM ammonium acetate buffer, pH 5.5), or cyt P450 2E1 (50 mL, 0.5 mg mL<sup>-1</sup>, 50 mM KH<sub>2</sub>PO<sub>4</sub>, pH 7.4) for 30 min followed by the same centrifugation and washing steps. For additional enzyme layers, PSS and enzyme deposition steps were repeated. Final films on the Si microbeads can be denoted in order of layer deposition as PDDA/(PSS/Enz)<sub>*n*</sub> (Enz = Mb, cyt P450<sub>cam</sub>, or cyt P450 2E1). These biocolloids are referred to as PDDA/PSS/Enz films.

For nucleobase adduct generation, PSS was replaced with layers of DNA (2 mg mL<sup>-1</sup>, 10 mM pH 7.1 Tris, 50 mM NaCl)

using the same procedure. In addition, a “capping” layer of DNA was added to the films to increase nucleobase reaction sites resulting in a final film architecture of PDDA/DNA/Enz/DNA. These films are denoted DNA/Enz.

**Myoglobin Activity Assay.** The activity of Mb was monitored by the method of Maehly and Chance.<sup>39</sup> PDDA/PSS/Mb colloids were resuspended in 1 mL of 10 mM pH 5.5 acetate buffer containing 4 mM guaiacol, and H<sub>2</sub>O<sub>2</sub> was added to 1 mM. Production of the colored product 3,3'-dimethoxy-4,4'-biphenyl-quinone<sup>39–41</sup> was monitored by UV–vis spectroscopy at 470 nm. The biocolloids were centrifuged from the reaction mixture before UV–vis spectra were obtained.

**Metabolite Detection. Safety note:** *Styrene, NNK, and their metabolites are suspected carcinogens. All procedures were done while wearing gloves and under closed hoods.* PDDA/PSS/Enz beads were resuspended in 0.5 mL of reaction buffer (10 mM sodium acetate, pH 5.5) containing either 1% styrene or 100 μM NNK with 1 mM H<sub>2</sub>O<sub>2</sub> and incubated at 37 °C for 30 s to 15 min. After styrene incubations, samples were extracted three times with 0.5 mL of hexane. The organic volume was then decreased to 0.2 mL under N<sub>2</sub>. An HP 6980 gas chromatograph (GC) equipped with a flame ionization detector (FID) was used for product analysis with methyl silicone RTX-5 (30 m × 0.32 mm i.d.) column, helium carrier gas, and temperature program 50–250 °C at 20 °C/min, then cooled to 50 °C at 40 °C/min.<sup>42</sup>

For product determination after NNK incubations, the reaction supernatant solution was injected directly into a capillary liquid chromatography (capLC) trapping column (see below) using an automated injection system.

**Nucleobase Adduct Detection.** Styrene oxide–guanine (Gua–SO) and styrene oxide–adenine (Ade–SO) adduct standards were prepared following a previous procedure.<sup>43</sup> DNA/enzyme biocolloids were exposed to the same reaction conditions as described above. After reactions, the bead dispersion was rinsed three times with hexane to remove excess styrene. The remaining aqueous medium containing the dispersed biocolloids was then subjected to neutral thermal hydrolysis for 15 min in boiling water,<sup>23</sup> followed by rapid cooling on ice. The hydrolysate was then filtered through a Centrion filter with 3000 MW cutoff (Amicon, Beverly, MA), and the filtered solution was analyzed by capLC–MS. These adducts were quantified by reference to a calibration curve developed using standards prepared as described earlier.<sup>43</sup>

DNA adducts formed from NNK metabolites were detected using similar procedures as for styrene adducts. The DNA/Enzyme biocolloids were exposed to 0.25 mL of 100 μM NNK + 1 mM H<sub>2</sub>O<sub>2</sub>. After incubation, reaction mixtures were centrifuged and the aqueous supernatant removed. DI water (250 μL) was added to the biocolloids, followed by neutral thermal hydrolysis for 15 min in boiling water,<sup>23</sup> then rapid cooling on ice. The hydrolysate was filtered as above and analyzed by capLC–MS.

**CapLC–MS/MS.** The analytical column was Atlantis dC18, 150 mm, 300 μm i.d., 5 μm particle size, and the trapping column was Atlantis dC18, 0.18 mm i.d., 5 μm particle size) from Waters. The capillary chromatograph system (Waters capLC–XE) allows the selective capture of desired adducts in the trapping column while discarding the rest of the injected sample to waste. A similar procedure as reported earlier was used.<sup>21,23</sup> Three 10 μL injections

(43) Tarun, M.; Rusling, J. F. *Anal. Chem.* **2005**, *77*, 2056–2062.

(44) Schenkman, J. B.; Jansson, I.; Lvov, Y.; Rusling, J. F.; Boussad, S.; Tao, N. *J. Arch. Biochem. Biophys.* **2001**, *385*, 78–87.

(45) Ueberfeld, J.; El-Difrawy, S. A.; Ramdhanie, K.; Ehrlich, D. *J. Anal. Chem.* **2006**, *78*, 3632–3637.

(46) (a) Lvov, Y. M.; Lu, Z.; Schenkman, J. B.; Zu, X.; Rusling, J. F. *J. Am. Chem. Soc.* **1998**, *120*, 4073–4080. (b) Zu, X.; Lu, Z.; Zhang, Z.; Schenkman, J. B.; Rusling, J. F. *Langmuir* **1999**, *15*, 7372–7377.

for each analysis were loaded into the trapping column at a flow rate of  $4.25 \mu\text{L min}^{-1}$  and washed with water for 2 min at  $10 \mu\text{L min}^{-1}$ . Trapped adducts were then back-flushed from the trapping column onto the analytical column at  $4.25 \mu\text{L min}^{-1}$  using the following elution gradient: 5 min–10% B, 10 min–10% to 30% B, 20 min–30% B, 5 min–30% to 10% B, 5 min–10% B. (A, 10 mM acetate buffer pH 5.5; B, methanol). Electrospray ionization mass spectrometry (ESI-MS) employed a Micromass Quattro II (Beverly, MA) operated in the positive ion mode (ESI<sup>+</sup>). Samples were analyzed in the single ion recording (SIR), single reaction monitoring (SRM), and total ion scan (TIC) modes. The cone voltage was 15 V, collision energy was 20 eV, and collision gas (Ar) pressure was  $5 \times 10^{-3}$  mbar.

**Quartz Crystal Microbalance.** Assembly of films on the microbeads was monitored at each step with a quartz crystal microbalance (QCM, USI Japan). Films were constructed on the beads, which were then adsorbed onto 9 MHz gold-coated QCM resonators (AT-cut, International Crystal Mfg., Oklahoma City, OK), and the solution was allowed to evaporate. This is similar to previously described procedures to monitor LbL film formation.<sup>19,46,47</sup> Layers were adsorbed into the microbeads in a similar manner as described above and then diluted 100 times in water followed by application of a  $2 \mu\text{L}$  droplet directly to the center of the resonator. The resonator was previously modified with several oppositely charged bilayers of PDDA and DNA to create a coated surface for more accurate frequency readings. The droplet was allowed to evaporate at  $40 \text{ }^\circ\text{C}$ , and then the frequency change was measured. Adsorbed mass (M/A) of each dried bead layer was obtained from the frequency change ( $\Delta F$ ) using the Sauerbrey equation for the 9 MHz resonators:<sup>25,26</sup>

$$M/A \text{ (g cm}^{-2}\text{)} = -\Delta F \text{ (Hz)} / 1.83 \times 10^8 \quad (1)$$

The gold resonators have a surface area of  $0.16 (\pm) \text{ cm}^2$ ;<sup>244</sup> therefore, the mass of the biocolloid layer was determined, and this provided a method to validate the bead stock solution and polymer/enzyme surface concentrations ( $\Gamma$ ). On the basis of the average frequency decrease, the volume, and density of the fused-silica microbeads, the factory stock solution was determined to be  $1.10 (\pm 0.30) \times 10^{12}$  microbeads  $\text{mL}^{-1}$  (factory supplied value  $7 \times 10^{11}$  microbeads  $\text{mL}^{-1}$ ).

**Atomic Force Microscopy.** Nominal thickness ( $d$ ) of the films was estimated using atomic force microscopy (AFM, Digital Instruments Nanoscope IV, tapping mode (TM)) to measure the diameter of the beads as layers of polymer and enzyme were added. Silicon AFM tips from Veeco Probes (model no. MPP-11100, symmetric tip, frequency 300 kHz, spring constant 40 N/m) were used. Samples were applied to the cleaved mica substrate in a similar manner as in QCM experiments and allowed to air-dry before imaging.

## RESULTS

**Biocolloid Characterization.** In order to ascertain proper layer formation and quantify the amount of enzyme on the beads, mass measurements after each layer application were done by QCM. After each layer was added to the beads, the sample was

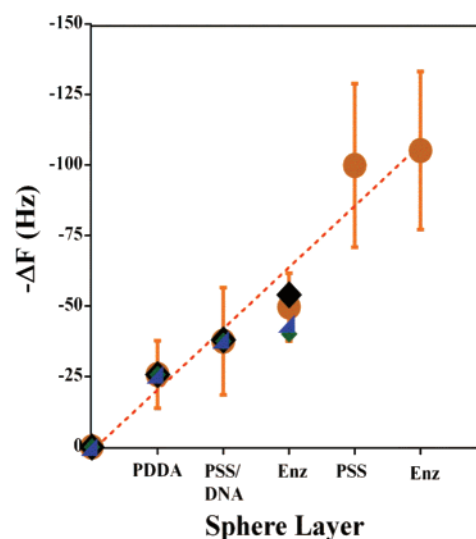


**Figure 1.** Influence of layers on microbeads on QCM frequency change. Films were adsorbed layer-by-layer on microbeads as PDDA/PSS/Mb/PSS/Mb (orange circles), PDDA/DNA/Mb (black squares), PDDA/PSS/cyt P450<sub>cam</sub> (blue triangles), and PDDA/PSS/cyt P450<sub>cam</sub> (green diamonds).  $\Delta F$  was measured after each adsorption step by deposition of  $2 \mu\text{L}$  of microbeads ( $500\times$  dilution from stock) on a QCM resonator. The error bars shown for PDDA/PSS/Mb/PSS/Mb were representative of all films for  $n = 5$  trials.

washed and a fixed amount was deposited on the QCM resonator and dried. Figure 1 shows QCM frequency decreases after subtracting the frequency change from the beads alone (Table 1) as a function of each layer applied to the beads. Table 1 summarizes the enzymatic surface coverage ( $\Gamma$ ) values obtained in this fashion. Cyt P450 2E1 was not employed in these experiments due to limited amounts of this human enzyme.

The amount of enzyme immobilized on the beads in  $\text{nmol cm}^{-2}$  determined from QCM was less than previously obtained QCM data determining the amount of Mb and cyt P450<sub>cam</sub> adsorbed on oppositely charged gold resonator surfaces.<sup>19–21</sup> The lower surface coverage on the beads could be a result of the nonfunctionalized nature of the silica versus that of a gold resonator. Also, with regard to cyt P450<sub>cam</sub>, the exposed surface area per nanomole is significantly less than when employing gold-coated QCM resonators. It is not surprising that the majority of cyt P450<sub>cam</sub> present in the solution would adsorb to this amount of beads (approximately  $2 \times 10^{11}$ ) as similar types of beads have been used effectively in the extraction of small amounts of biomaterial.<sup>45</sup>

These data demonstrate that we adsorb a similar amount of enzyme on the bead regardless of the oppositely charged polyion used (DNA or PSS) in approximate agreement with our previous work on macroscopic surfaces.<sup>47</sup> The relatively large standard deviation using the QCM method is most likely due to numerous factors including the localization of the  $2 \mu\text{L}$  droplet, which does not dry over the entirety of the gold resonator, and variability in biocolloid dispersions upon layer applications, separations, and reconstitution.

To verify the QCM analyses, UV–vis absorbance was employed. Spectra of the Mb and cyt P450<sub>cam</sub> solutions used to form the layers on the beads were obtained before and after exposure to the beads (Figure S7, Supporting Information). By comparing absorbance change in the Soret band for Mb (409 nm) and both high- and low-spin absorbance values for cyt P450<sub>cam</sub> (392 and

(47) Munge, B.; Estavillo, C.; Schenkman, J. B.; Rusling, J. F. *Chem. Biochem.* **2002**, *4*, 101–108.

**Table 1. Film Surface Concentrations ( $\Gamma$ ) and Masses for PDDA/DNA/Enz/DNA and PDDA/PSS/Enz Films from QCM and Spectroscopy**

method	bead mass ( $\mu\text{g}$ ) <sup>a</sup>	DNA mass (fg) <sup>b</sup>	PSS mass (fg) <sup>b</sup>	$\Gamma$ Mb (PSS) <sup>c</sup>	$\Gamma$ Mb (DNA) <sup>c</sup>	$\Gamma$ cyt P450 <sub>cam</sub> (PSS) <sup>c</sup>	$\Gamma$ cyt P450 <sub>cam</sub> (DNA) <sup>c</sup>
QCM	$0.50 \pm 0.20$	$2.1 \pm 0.9$	$2.1 \pm 0.6$	$16 \pm 8$	$21 \pm 6$	$1.3 \pm 0.7$	$2.8 \pm 1.3$
absorbance				$23 \pm 5$	$18 \pm 4$	$0.74 \pm 0.20$	

<sup>a</sup> Mass of 2  $\mu\text{L}$  of diluted silica microbead application to gold-coated QCM resonator, which equates to  $\sim 5 \times 10^6$  beads. <sup>b</sup> Mass per bead. <sup>c</sup> pmol  $\text{cm}^{-2}$ ; polymer in parentheses is that used in the films with that specific enzyme.

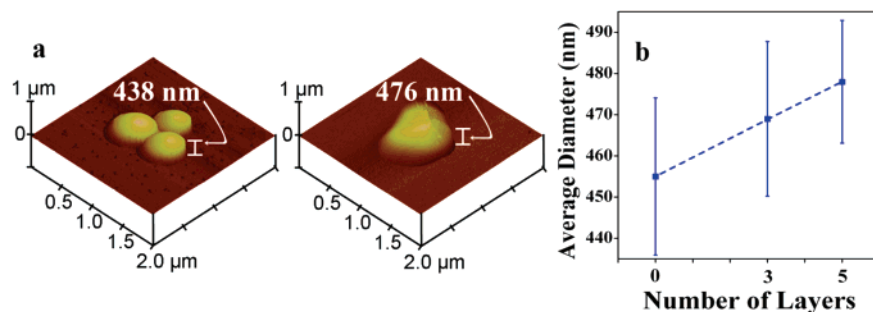


**Figure 2.** (a) TMAFM images of representative bare microbeads (left image) and microbeads modified with PDDA/(PSS/Mb)<sub>2</sub> layers (right image). (b) Average diameter increase upon adding polymer/enzyme layers starting with bare microbeads (0), PDDA/PSS/Mb-coated beads (3), and PDDA/(PSS/Mb)<sub>2</sub> beads (5). The error bars shown represent standard deviations for respective layers.

417 nm, respectively) before and after use for layer deposition, the amount of immobilized enzyme was ascertained. High- and low-spin absorption bands were seen in the cyt P450<sub>cam</sub> spectra due to the presence of some camphor used to stabilize the enzyme during storage in solution.  $\Gamma$  estimated in this way is also summarized in Table 1 and provides values that agree within experimental error with those obtained using QCM.

Atomic force microscopy was used to estimate particle size and nominal film thicknesses. For AFM, dilute solutions of unmodified and coated microbeads were deposited onto a clean mica surface and allowed to dry. Areas of the surface were then scanned with the probe tip, looking for isolated, nonaggregated beads.

Figure 2a demonstrates that the microbeads did indeed increase in diameter upon adsorption of polymer and enzyme layers. These modified microbeads show approximately 40 nm growth upon addition of PDDA/(PSS/Mb)<sub>2</sub> layers. This behavior is demonstrated graphically in Figure 2b, which plots the average diameter of the beads with each applied polymer/enzyme layer. Error bars represent an approximate 10% variance in layer film thicknesses. The average diameter of the bare microbeads from AFM was  $455 \pm 19$  nm, which is within the manufacturer stated value of  $500 \text{ nm} \pm 10\%$ . The diameter increased  $\sim 5$  nm after each layer was deposited, which is expected based on layer thicknesses when using high saline polymer solutions and the thickness of Mb layers ( $\sim 5$  nm) in previous reports.<sup>19,21,46</sup>

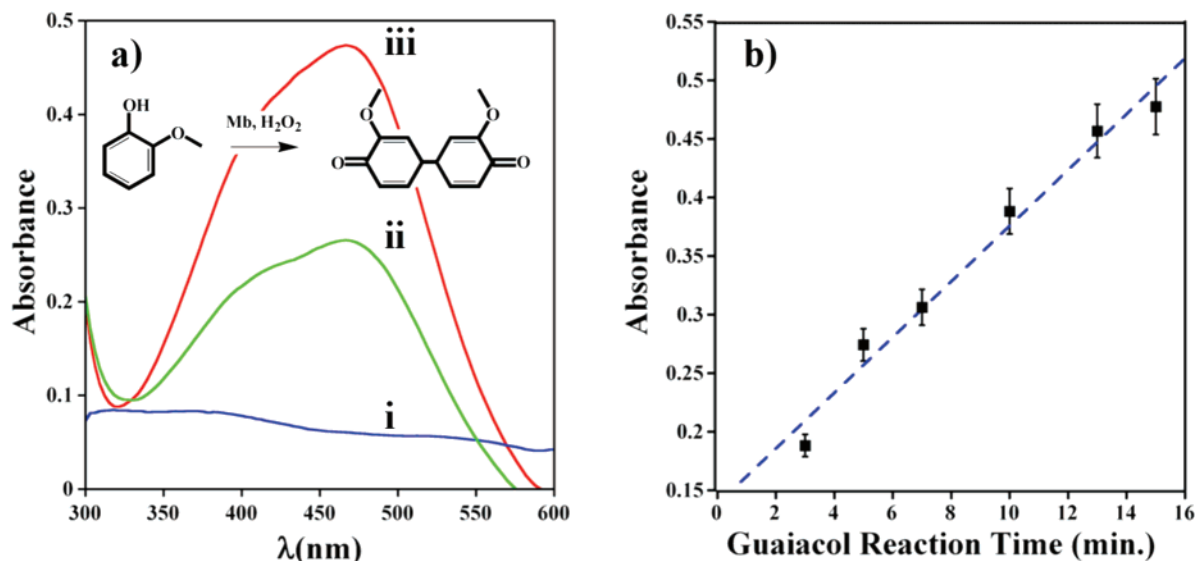
**Myoglobin Activity Assay.** The activity of immobilized Mb was initially characterized using the oxidation of classic peroxidase substrate guaiacol activated by hydrogen peroxide to generate the colored dimer product, 3,3'-dimethoxy-4,4'-biphenylquinone ( $\lambda_{\text{max}} = 470 \text{ nm}$ ).<sup>39,41</sup> This provided a facile method to verify that Mb adsorbed on the biocolloids was active and to ascertain the nature of multiple layers of enzyme on the beads. Figure 3a shows the absorbance of reaction solutions after 10 min. The absorbance at  $\lambda = 470 \text{ nm}$  is due to the product (see Figure 3a, inset). The

absorbance approximately doubles when doubling the amount of Mb by adding a second layer onto the biocolloids. This shows that Mb retains its peroxidase activity on the beads and demonstrates that Mb activity is proportional to the amount of enzyme present, i.e., outer layers do not influence the reactivity of the inner layers in these very thin films.

Figure 3b shows a linear absorbance increase at 470 nm with reaction time. This suggests that 1 mM H<sub>2</sub>O<sub>2</sub> does not significantly alter the activity of the Mb over this time period, which is consistent with previous reports concerning stability of film-immobilized enzymes.<sup>46,47</sup> For comparison, similar concentrations of Mb in solution were exposed to guaiacol and hydrogen peroxide for up to 30 min and spectra were recorded (Supporting Information, Figure S1). These data show that similar activity was obtained from biocolloidal and solution-phase Mb.

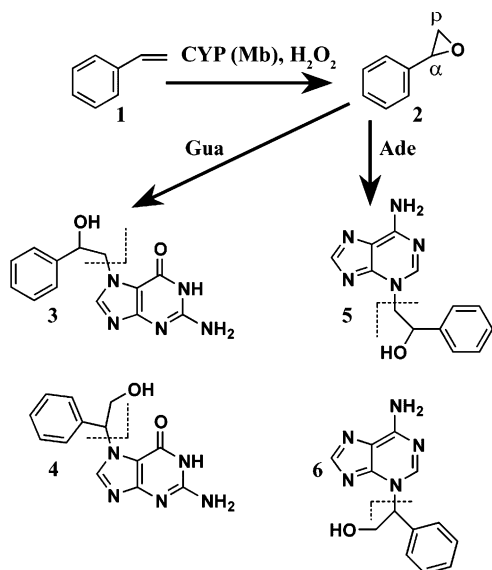
**Detection of Reactive Metabolites.** Biocolloids coated with cyt P450<sub>cam</sub> did not catalyze oxidation of guaiacol. We previously showed that films of cyt P450<sub>cam</sub> and Mb on gold or carbon electrodes catalytically oxidize styrene to styrene oxide when activated by hydrogen peroxide as illustrated at the top of Scheme 2.<sup>46,47</sup> Figure 4a shows GC chromatograms of hexane-extracted reaction mixtures after exposure to either cyt P450<sub>cam</sub> or Mb biocolloids (no DNA) as well as a control with no enzyme. The figure shows major peaks at retention times 4 and 6.3 min. The 6.3 min peak is due to styrene oxide and the 4 min peak is due to styrene, while the small peak at 5.9 min is styrene glycol from hydrolysis of styrene oxide, facilitated by the slightly acidic conditions. Confirmation of the products arises through gas chromatography/mass spectrometry (GC/MS) comparison with standards (Supporting Information, Figure S2).

Figure 4b shows that the amount of styrene oxide produced per nanomole of enzyme increased linearly with reaction time. The surface area of one silica bead is approximately  $1.26 \times 10^{-9} \text{ cm}^2$ , and we employ approximately  $2 \times 10^{11}$  beads for each reaction. Therefore, on the basis of the surface coverage from



**Figure 3.** Results of oxidation of 4 mM guaiacol in pH 5.5 buffer catalyzed by Mb-coated biocolloids activated with 1 mM  $\text{H}_2\text{O}_2$ : (a) visible spectra of the reaction medium 10 min after removing biocolloids by centrifugation (i) using PDDA/PSS microbeads (no Mb); (ii) using PDDA/PSS/Mb; (iii) using PDDA/(PSS/Mb)<sub>2</sub>. The guaiacol oxidation reaction is shown in the inset. (b) Influence of time on absorbance at 470 nm of the above reaction medium. The error bars represent standard deviations for  $n = 3$  trials.

### Scheme 2. Enzymatic Catalysis of Styrene Oxide Formation (2) from Styrene (1)<sup>a</sup>



<sup>a</sup> Styrene oxide reacts with guanine (Gua) and adenine (Ade) at either the  $\alpha$ - or  $\beta$ -carbon (denoted) of the epoxide to form primarily N7-Gua adducts ( $\beta$ -3;  $\alpha$ -4) or N3-Ade adducts ( $\beta$ -5;  $\alpha$ -6). Dashed lines demonstrate locations of fragmentation for MS analysis.

QCM (Table 1), amounts of Mb and cyt P450<sub>cam</sub> present in each experiment were approximately 31 and 3 nmol, respectively. These data were used to determine enzyme turnover rates summarized in Table 2. Slightly more styrene oxide was produced per min from Mb films; however, approximately 10 times more Mb was present on the beads compared to cyt P450<sub>cam</sub> (Table 2). Therefore, the relative turnover of cyt P450<sub>cam</sub> biocolloids was much higher than that from Mb, which correlates well with previous studies using LbL films on macroscopic surfaces.<sup>46,47</sup>

In comparison to our previous work employing carbon cloth to immobilize Mb and detect reactive metabolites,<sup>43</sup> the amount

of styrene oxide produced in a similar amount of time from the biocolloids represents a 3-fold increase (2.7 vs 0.816 nmol min<sup>-1</sup>). This increase is due to the increase in reactive surface area containing Mb. The carbon cloth squares previously used had an approximate surface area of 600–700 cm<sup>2</sup>. Here, the total surface area approaches 1600 cm<sup>2</sup>, representing an approximate 2.5-fold increase, which correlates well with the ~3-fold increase in rate of product formation. Also, reaction volume with the biocolloid catalysts was decreased to 0.5 mL compared to ~50 mL needed to cover the typical-sized carbon cloth, and the ease in handling the biocolloids compared to highly porous carbon cloth resulted in better quality extractions and more reliable product recovery.

**Detection of Styrene Oxide Nucleobase Adducts.** The DNA/Enz biocolloids were used to generate DNA nucleobase adducts from reactions with metabolites. Styrene oxidation was done as described above followed by neutral thermal hydrolysis to obtain a sample enriched in damaged nucleobases. This involves heating the beads in water to selectively eject damaged bases from DNA in the films.<sup>22,43</sup>

Figure 5a shows a partial LC chromatogram in TIC mode obtained after a 10 min of reaction catalyzed by Mb- and cyt P450<sub>cam</sub>-DNA biocolloids. Two sets of nascent peaks are seen, which are attributed to adenine-styrene oxide (Ade-SO, 30 min) and guanine-styrene oxide (Gua-SO, 35 min) adducts. Calibration standards for Ade-SO and Gua-SO (Supporting Information, Figure S3) were used to identify and quantify the amounts of Ade-SO and Gua-SO formed in situ as depicted in Figure 5a. Two sets of peaks arise for each adducted base due to the reaction of both  $\alpha$  and  $\beta$  epoxide carbons on the nucleobase (Scheme 2). The  $\beta$ -N7-guanine adduct has been shown to be the primary and latest eluting of the two N7 Gua-SO adducts,<sup>14</sup> which is consistent with Figure 5.

Figure 5b shows plots of total amounts of Gua-SO and Ade-SO adducts detected in reactions catalyzed by Mb and cyt P450<sub>cam</sub> versus reaction time. Amounts of nucleobase adducts increased

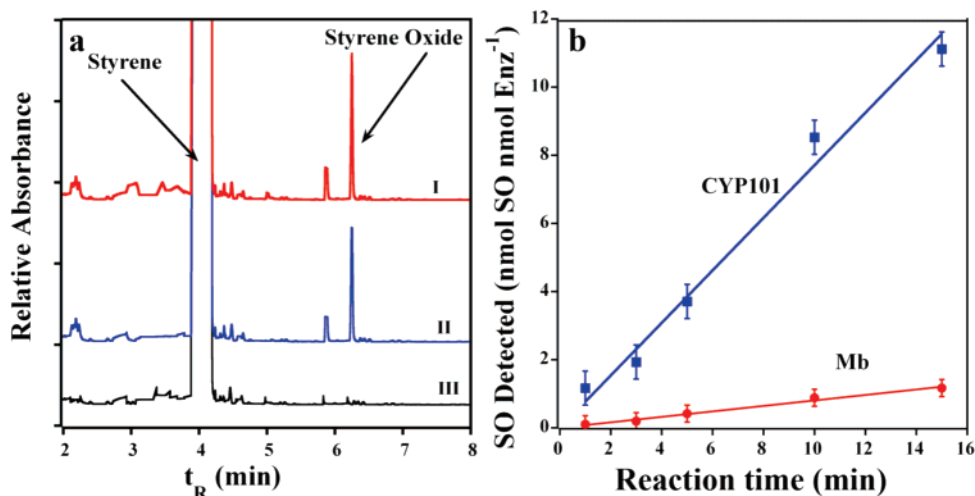


**Figure 4.** GC results for extracted reaction media (a) after 10 min of treatment with 1% styrene and 1 mM H<sub>2</sub>O<sub>2</sub> in pH 5.5 buffer of (I) PDDA/PSS/Mb beads, (II) PDDA/PSS/cyt P450<sub>cam</sub> beads, and (III) PDDA/PSS control beads. (b) Influence of reaction time on the amount of styrene oxide (SO) produced per mole of immobilized enzyme (circles = Mb; squares = cyt P450<sub>cam</sub>). The error bars represent standard deviations.

**Table 2. Metabolite and DNA Adduct Formation Rates as Relative Turnover Numbers Using Biocolloids (see the Experimental Section for Details)**

	Mb	cyt P450 <sub>cam</sub>	cyt P450 2E1
styrene oxide <sup>a</sup>	81 ± 12	770 ± 110	1270 ± 320
HPB <sup>a</sup>			940 ± 90
Gua-SO <sup>b</sup>	22 ± 3.0	174 ± 19	
Ade-SO <sup>b</sup>	1.9 ± 0.6	15 ± 4	
total adduct rate <sup>b</sup>	24 ± 3	190 ± 19	
% adducts <sup>c</sup>	0.030 ± 0.004	0.025 ± 0.004	

<sup>a</sup> pmol product (nmol Enz)<sup>-1</sup> min<sup>-1</sup>. <sup>b</sup> fmol total adducts (nmol Enz)<sup>-1</sup> min<sup>-1</sup>. <sup>c</sup> As percent of reactive intermediate formed.

linearly over ~5 min of reaction, with guanine adducts produced at a much faster rate. The slopes of these plots were used to estimate relative enzyme turnover rates (Table 2). Figure 5b shows that the production of the adducted nucleobases is greater with cyt P450<sub>cam</sub>, ~10 times higher than for Mb, consistent with the metabolite formation rate (cf., Figure 4b).

Adducts detected in Figure 5 were further analyzed by tandem mass spectrometry (MS/MS) in SRM mode with the assumption that the detected species in the TIC chromatograms have [M + H]<sup>+</sup> of a nucleobase with a pendant styrene oxide moiety (cf., Scheme 3).<sup>23</sup> In addition, collision-induced dissociation (CID) of standard Ade-SO and Gua-SO solutions prepared by reacting styrene oxide with either adenine or guanine provided the standard adduct masses.<sup>23</sup> Based on these considerations, we monitored SRM transitions of the adduct nucleobases for *m/z* 256 (Ade-SO) → *m/z* 136 (Ade) and *m/z* 272 (Gua-SO) → *m/z* 152 (Gua) consistent with fragmentation of the expected styrene oxide-nucleobase adducts. Figure 6a shows the SRM product ion chromatograms for both transitions, and Figure 6, parts b and c, shows the mass spectra. These data are consistent with the structures and fragmentation patterns of the adducts in Scheme 2. Comparison of the SRM peak retention time to those of the TIC chromatogram demonstrates that the peaks seen in Figure 5 can indeed be assigned to styrene oxide adducts of adenine and guanine.

**Metabolites and DNA Adducts from Cyt P450 2E1 Catalysis.** To demonstrate the versatility of the biocolloid approach, styrene oxide and NNK were oxidized using human cyt P450 2E1 immobilized on biocolloids. Cyt P450 2E1 is a prime catalyst in the metabolism of styrene in vivo.<sup>11b,48</sup> NNK is an *N*-nitroso procarcinogenic representative of compounds in cigarette smoke and has been implicated in cancer risk among smokers.<sup>49,50</sup> Hecht and co-workers elucidated metabolic pathways of NNK,<sup>31,49,51</sup> and we recently detected DNA damage by metabolites of *N*-nitrosopyrrolidine (NPYR) by cyt P450 2E1 using ECL sensor arrays.<sup>29</sup>

Styrene and NNK were reacted with PSS/cyt P450 2E1 biocolloids activated by 1 mM H<sub>2</sub>O<sub>2</sub>. Cyt P450-catalyzed metabolites of NNK undergo hydrolysis forming HPB, which is the actual species detected under these reaction conditions<sup>49</sup> (Scheme 3). Figure 7 shows styrene oxide and HPB production as detected by GC (styrene oxide) or LC-MS in TIC mode (HPB). The production of both metabolites increased with time up to 10 min. Sample chromatograms are shown in Supporting Information, Figure S4. Quantification of peak areas for HPB analysis was done using an HPB calibration curve (Supporting Information, Figure S5).

Limited expression levels<sup>11a</sup> of human P450 2E1 did not allow enough enzyme for a full QCM measurement and  $\Gamma$  determination on the microspheres. However, based on previous QCM data for similar P450 2E1 films on flat gold resonators,<sup>29</sup> we estimate the amount of this enzyme at about half that of cyt P450<sub>cam</sub>. With the use of this approximation, apparent rates of formation are 1.27 nmol styrene oxide and 0.94 nmol HPB (nmol cyt P450 2E1)<sup>-1</sup> min<sup>-1</sup> (Table 2).

DNA/cyt P450 2E1 biocolloids were used for generation and detection of DNA adducts from NNK metabolites. Figure 8 shows

(48) Tanaka, E.; Terada, M.; Misawa, S. *J. Clin. Pharm. Ther.* **2000**, *3*, 165–175.

(49) Wang, M.; Cheng, G.; Sturla, S. J.; Shi, Y.; McIntee, E. J.; Villalta, P. W.; Upadhyaya, P.; Hecht, S. S. *Chem. Res. Toxicol.* **2003**, *16*, 616–626.

(50) Hecht, S. S. *Nat. Rev. Cancer* **2003**, *10*, 733–744.

(51) Sturla, S. J.; Scott, J.; Lao, Y.; Hecht, S. S.; Villalta, P. W. *Chem. Res. Toxicol.* **2005**, *18*, 1048–1055.

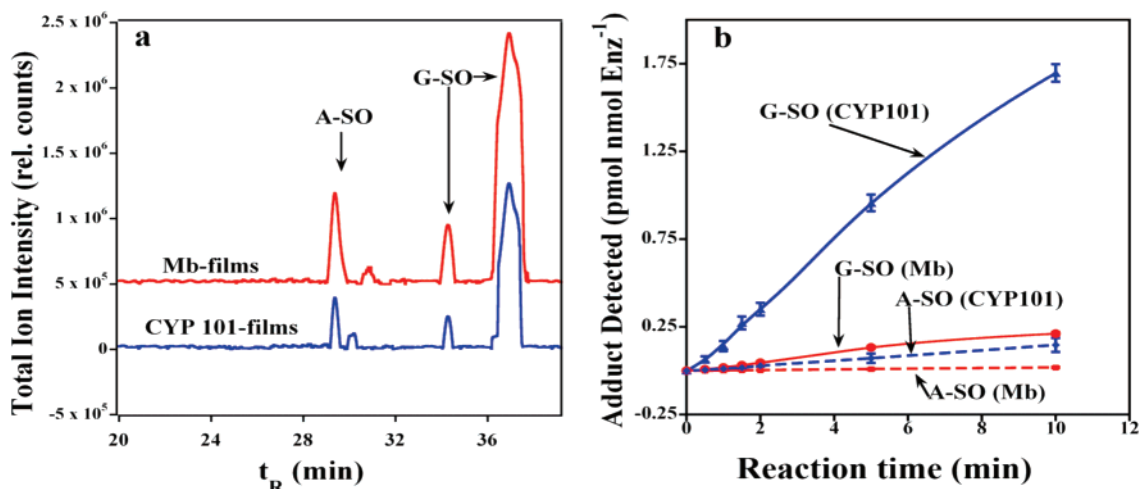
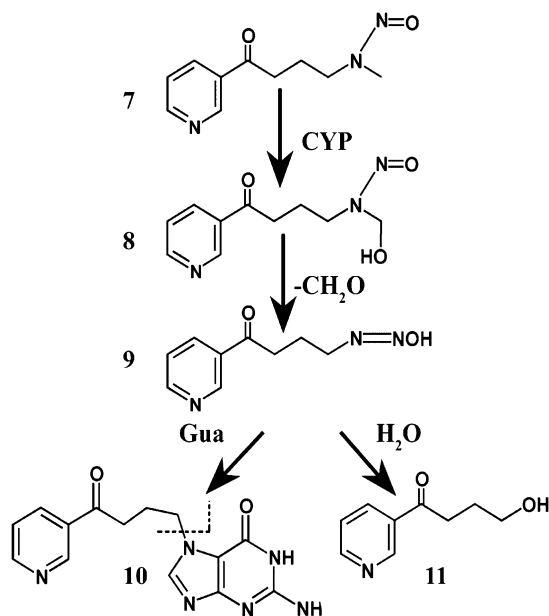


**Figure 5.** Detection of styrene oxide–nucleobase adducts with DNA/Enz biocolloids. (a) capLC–MSTIC chromatogram of filtered hydrolysate obtained after neutral thermal hydrolysis of denoted DNA/Enz biocolloids following reactions in pH 5.5 buffer with 1% styrene + 1 mM H<sub>2</sub>O<sub>2</sub>. (b) Influence of reaction time on the amount of guanine–styrene oxide (Gua–SO) and adenine–styrene oxide (Ade–SO) adducts detected per mole of enzyme. The error bars represent standard deviations.

### Scheme 3. Pathway for Cyt P450-Catalyzed NNK Bioactivation of NNK (7) (Ref 49)<sup>a</sup>



<sup>a</sup> NNK undergoes  $\alpha$ -hydroxylation to short-lived intermediate (**8**) that loses formaldehyde to form 4-oxo-4-(3-pyridyl)-1-butanediazohydroxide (**9**). Reaction of **9** with guanine produces several adducts. Shown is pyridyloxobutylation at N7 (**10**, 7-[4-oxo-4-(3-pyridyl)but-1-yl]Gua). In addition, hydrolysis of **9** produces 4-hydroxy-1-(3-pyridyl)-1-butanone (HPB, **11**). The dashed line in **10** represents fragmentation in MS.

the capLC–MS/MS chromatogram and spectrum obtained (SRM) showing the elution and corresponding  $m/z$  of nascent product peaks seen after reaction and workup. We monitored  $m/z$  299→152 as this is consistent with the previously reported pyridyloxobutylation of guanine via attachment at the most likely N7 location (Scheme 3).<sup>49</sup> After neutral thermal hydrolysis of the sample, we expected that pyridyloxobutylated N7-guanine adducts would give rise to peaks at  $m/z$  299.<sup>49</sup> Scheme 3 illustrates the expected fragmentation of an N7-pyridyloxobutylated guanine that

would produce  $m/z$  152 (Gua) upon fragmentation, which is consistent with data in Figure 8.

The multiple peaks in Figure 8a are likely due to several positional isomers,<sup>49</sup> since monitoring at this  $m/z$  also detects adducts with linkages to other guanine atoms. In any case, species with  $m/z$  299 present in the hydrolysate are consistent with the formation of pyridyloxobutyl–guanine from the cyt P450-catalyzed oxidation of NNK. Figure S6 in the Supporting Information shows the TIC chromatogram and MS obtained for the hydrolysate upon neutral thermal hydrolysis of the DNA/cyt P450 2E1 films. The figure demonstrates a significant set of peaks arising at  $\sim$ 37 min with predominant  $m/z$  299, consistent with the expected pyridyloxobutyl–guanine adducts.

In this case, HPB is not the DNA-reactive metabolite. The precursor to HPB is a short-lived species that reacts with DNA (**9**, Scheme 3). Because of the reactivity of this intermediate, we were not able to obtain appropriate adduct standards or quantify the  $m/z$  299 peak. However, Figure 8c shows that the integrated area of this peak increases linearly similar to HPB in Figure 7. This suggests that the amount of specific metabolite produced mirrors the amount of predominant DNA adducts in the films.

## DISCUSSION

Results above show that biocolloids made by coating silica microbeads with enzymes or enzymes and DNA offer excellent tools for studies of enzyme kinetics and DNA adduct formation. Advantages include larger enzyme activities, conservation of enzyme, better reactivity and yields, ease of sample handling, and tiny adsorbate and reaction volumes compared to earlier efforts with similar films on carbon cloth.<sup>22,43</sup> In comparison to traditional solution methods for DNA adduct formation detection, enzyme–DNA biocolloids generate metabolic products in environments densely packed with reactive nucleobases and provide significantly more DNA adducts in several minutes. In the case of Mb and cyt P450<sub>cam</sub> reacting with styrene, we were not able to obtain any nucleobase adducts in comparable reaction times with all components in solution.

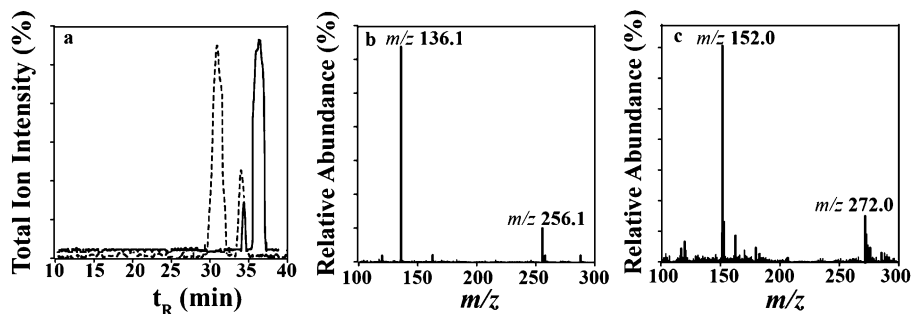


**Figure 6.** Partial SRM capLC chromatogram of the styrene reaction mixture after catalysis with cyt P450<sub>cam</sub> biocolloids (a) measuring  $m/z$  256  $\rightarrow$  136 (dashed line, Ade-SO  $\rightarrow$  Ade) and  $m/z$  272  $\rightarrow$  152 (solid line, Gua-SO  $\rightarrow$  Gua) and tandem mass spectra (b and c) from the resulting peaks in (a). The chromatograms in (a) are slightly offset for clarity.

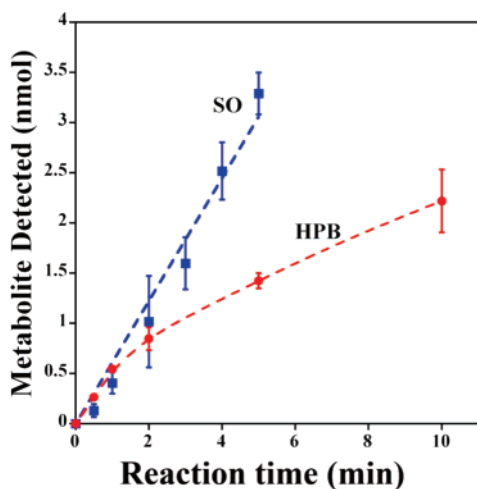


**Figure 7.** Influence of reaction time on the amount of styrene oxide (squares) from 1% styrene and HPB (circles) from 100  $\mu$ M NNK found during catalysis by PSS/cyt P450 2E1 colloids activated by 1 mM H<sub>2</sub>O<sub>2</sub> in pH 5.5 buffer. The error bars represent standard deviations.

Although smaller colloids might be used in these applications, we chose to use 500 nm diameter silica beads because of ease of handling and centrifugal separation. Preliminary studies with 45 nm silica nanoparticles led to aggregation during film formation and separation steps. Thus, combined with the high sensitivity of modern capLC-MS/MS, the 500 nm particles provide sufficient amounts of desired products so that turnover rates for metabolite or DNA adduct formation can be estimated in <5 min of reaction time.

The surface area of each 500 nm silica particle is  $\sim 8 \times 10^{-9}$  cm<sup>2</sup> with a volume of  $\sim 10^{-14}$  cm<sup>3</sup>. This equates to approximately 7600 cm<sup>2</sup> of reactive surface area per mL of dispersed particles ( $d = 1.96$  g/cm<sup>3</sup>). Due to their small total volume, the volume containing adsorbed enzymes during biocolloid preparation can also be very small ( $\sim 500$  times smaller than previous reports).<sup>23</sup> Further, in the smallest reaction volume of 0.25 mL used here, the total amount of cyt P450 on the beads (Table 1) was 2–5 nmol. Such biomaterial economy is an important consideration when valuable or rare enzymes are used and extends the scope of biologically relevant reactions that can be studied.

The small volume requirement for biocolloid preparation allows immobilization of bacterial and human cyt P450 isoforms obtainable only in limited amounts. The subsequent monitoring of

genotoxicity-causing DNA damage produced by reactive metabolites is a significant step toward incorporating virtually any human cyt P450 enzyme onto biocolloids for drug development and genotoxicity studies. Cyt P450 2E1 is significant in human drug and xenobiotic metabolism,<sup>4,48,52</sup> and its inclusion demonstrates viable real-world applicability of this method for metabolic and genotoxicity evaluations.

Data presented in Figure 1 and Table 1 demonstrate that the electrostatic LbL assembly can be achieved on the microbeads in similar ways to macroscopic surfaces<sup>19,21,29</sup> for these enzymes and DNA. QCM frequency shifts demonstrate reproducible layer formation, and AFM (Figure 2) showed consistent diameter increases upon adsorption of the layers. A smaller overall enzyme surface concentration, compared to carbon and gold surfaces used previously,<sup>19,21,29</sup> was compensated by larger active surface area and small reaction volumes to provide significantly increased metabolite and DNA adduct production for subsequent analysis.

Enzyme activity assays employing guaiacol dimerization (Figure 3) and styrene and NNK oxidation (Figures 4 and 7) showed that Mb, cyt P450<sub>cam</sub>, and cyt P450 2E1 retain high catalytic activity when bound on the silica beads. The guaiacol assay results showed that several layers of enzyme on the colloidal surface do not preclude the reactivity of the inner layers. We kept the number of enzyme layers at 2 to avoid mass transport limitations identified with thicker films on macroscopic surfaces.<sup>47</sup>

Figures 4–8 demonstrate that enzymes on the silica beads activated by hydrogen peroxide produce measurable reactive metabolites of styrene oxide and NNK within several minutes. A key feature of the approach is that rates of metabolite generation (Figures 4 and 7) and DNA damage (Figures 5 and 8) are easily measured, as discussed in more detail below. Based on the amount of enzyme present in the biocolloids (Table 1), we estimated that cyt P450<sub>cam</sub> is  $\sim 10$  times more active for styrene oxidation than Mb (Table 2). This is consistent with our previous studies for films of these enzymes on macroscopic surfaces.<sup>47</sup> Cyt P450 2E1 has a slightly larger catalytic activity for styrene oxidation than cyt P450<sub>cam</sub> and a much larger one than Mb (Table 2). These turnover rates are consistent with reports that cyt P450 2E1 is efficient in the *in vivo* metabolism of styrene.<sup>48</sup> The turnover rate that cyt P450 2E1 exhibits toward NNK is approximately equal to styrene oxide. However, substrate concentration was 100  $\mu$ M NNK compared to  $\sim 10$  mM styrene, so the effective reaction rate for NNK is much larger. Once again, this high rate of turnover is consistent with reports of the importance of cyt P450 2E1 as a

(52) Gonzalez, F. J. *Drug Metab. Dispos.* **2006**, *35*, 1–8.

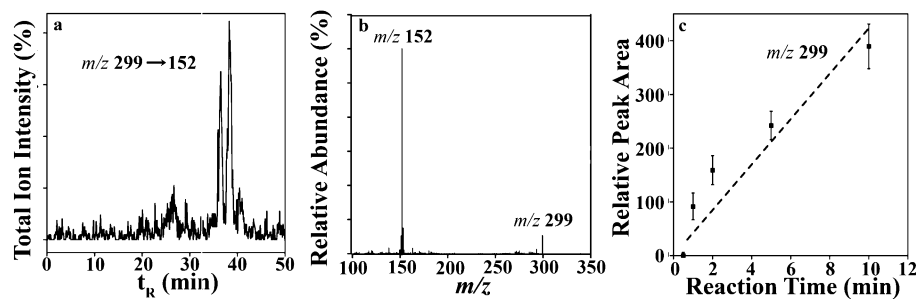


**Figure 8.** CapLC–MS/MS results for the NNK reaction medium catalyzed by DNA/cyt P450 2E1 microbeads in pH 5.5 buffer. (a) Chromatogram after 15 min of reaction; (b) mass spectrum analyzed by SRM ( $m/z$  299  $\rightarrow$  152) of the same sample as in (a); (c) influence of reaction time on total integrated area of the peaks in (a) at  $t_R = 37$ . The error bars represent standard deviations.

key cyt P450 isoform in the *in vivo* metabolism of NNK.<sup>31,53,54</sup> Note that this is not a biological assay but, rather, is designed to be complementary to such assays. In this light, the promutagen exposure concentrations can be selected at a level to facilitate detecting the primary adducts.

We previously reported<sup>23</sup> a 30 fmol detection limit of N7-guanine–styrene oxide adducts by capLC–MS/MS and a damage rate of approximately 0.57 nM guanines  $\text{min}^{-1}$  using films on carbon cloth. Using the biocolloids, we confirmed the N7-guanine adduct (Scheme 2) detection limit representing signal-to-noise (S/N) of 3:1 at 30 fmol but found a damage rate of 2.6 nM guanines  $\text{min}^{-1}$ , a 4-fold increase over the rate reported previously.<sup>23</sup> This is a direct consequence of the larger enzyme activity of the biocolloid system. In addition, we detected adenine–styrene oxide adducts and measured their formation rates using the biocolloids, which was not possible with Mb/DNA films on carbon cloth.

CapLC–MS/MS provided identification of nucleobase adducts ejected from the biocolloid films with  $m/z$  consistent with both adenine and guanine attached to styrene oxide (Scheme 2, Figures 5 and 6, and Table 2). The ratio of SO–Gua adducts to SO–Ade adducts detected was consistent with previous literature findings. Hemminiki reported that two N7-guanine (7-(2-hydroxy-1-phenylethyl)-guanine or 7-(2-hydroxy-2-phenylethyl)-guanine) and two N3-adenine (3-(2-hydroxy-1-phenylethyl)-adenine or 3-(2-hydroxy-2-phenylethyl)-adenine) positional isomers were formed in a ratio of 25:1 (Gua to Ade) upon exposure of styrene oxide to st-DNA in solution.<sup>14</sup> Here we found that the adducts were formed in 13:1 and 12:1 Gua-to-Ade ratios for Mb and cyt P450<sub>cam</sub> films, respectively (Table 2). These ratios demonstrate a higher percentage of adenine adducts. It is likely that the high concentration of DNA and enzymes offered in biocolloid format increases formation rates of adenine adducts leading to a lower Gua–SO to Ade–SO ratio.

Styrene oxide forms at least 10 different adducts with DNA bases, along with positional isomers due to reaction at both the  $\alpha$  and  $\beta$  epoxide carbons of styrene oxide (Scheme 2).<sup>14</sup> The clear majority of these adducts (approximately 97% formed *in vitro*) are the N7 and N3 guanine and adenine adducts, respectively.<sup>55</sup> In our previous work with Mb–DNA films on carbon cloth,<sup>23</sup> we were able to detect only the major adducts, *i.e.*, those of guanine. Use

of the biocolloids enabled production of enough of the minor adducts, those of adenine, in short reaction times so that they were also detected (Table 2). The products of these reactions on the microspheres were confirmed through comparison and calibration with appropriate SO–DNA standards.

From cyt P450 2E1-catalyzed oxidation of NNK, we were able to identify  $[M + H]^+ m/z$  299  $\rightarrow$  152, which is consistent with the pyridyloxobutylation of guanine sites likely resulting in 7-[4-oxo-4-(3-pyridyl)but-1-yl]Gua adducts (Scheme 3, Figure 8) formed in the suggested metabolic pathway.<sup>49</sup> NNK undergoes cyt P450-catalyzed  $\alpha$ -hydroxylation (Scheme 3) either at the methyl or methylene forming an array of reactive metabolites and DNA adducts. Hydroxylation at the NNK terminal methyl group (**8**, Scheme 3) eventually yields reactive 4-oxo-4-(3-pyridyl)-1-butanone (HPB, **11**, Scheme 3).<sup>49</sup> Multiple peaks near the 37 min retention time in the SRM chromatogram (Figure 8a) most likely reflect formation of multiple adduct isomers consistent with reports by Hecht and co-workers.<sup>31,49</sup> However, we can infer that the N7 guanine adduct represents a significant portion of the detected adducts. The N7 adduct (**10**, Scheme 3) identified by Wang *et al.*<sup>49</sup> is thermally unstable and represented 35% of the adducts identified after neutral thermal hydrolysis. They also identified an unknown adduct with similar  $m/z$ ,<sup>49</sup> which may also contribute to the  $m/z$  299  $\rightarrow$  152 peak area shown in Figure 8a. The rate in HPB production (Figure 7) mirrors the rate of  $m/z$  299 peak area increase (Figure 8c), suggesting that the rate of production of NNK metabolites reflects the amount of DNA adducts detected.

GC analysis showed that cyt P450<sub>cam</sub> was approximately 10 times more active in producing reactive styrene oxide from styrene exposure with a similar trend in DNA adducts detected from the films compared to Mb films (Table 2). Based on rates of metabolite and total DNA adducts formation with cyt P450<sub>cam</sub> and Mb films, we estimate that approximately 0.03% of the reactive metabolites undergo reactions resulting in a DNA adduct under these conditions. On the basis of previous reports,<sup>14</sup> neutral thermal hydrolysis provides collection and preconcentration of 90% of the styrene oxide DNA adducts formed in the films, lending confidence to the accuracy of this estimate.

(53) Abdel-Rahman, S. Z.; Salama, S. A.; Au, W. W.; Hamada, F. A. *Pharmacogenetics* **2000**, *10*, 239–249.

(54) Crespi, C. L.; Penman, B. W.; Gelboin, H. W.; Gonzalez, F. J. *Carcinogenesis* **1999**, *12*, 1197–1201.

(55) Koskinen, M.; Vodicka, P.; Hemminki, K. *Chem.–Biol. Interact.* **2000**, *124*, 13–17.

In summary, enzyme–DNA-coated microbeads provide significant improvements in reactive surface area and decreases in reaction volume over alternative methods to provide a superior procedure for DNA adduct detection from reactive metabolites. This approach enables the use of relevant human liver cyt P450 enzymes in limited quantities to measure relative rates of formation of major and minor DNA adducts as well as the metabolites themselves. Preliminary studies have also shown that liver microsomes can be used as the enzyme source in these biocolloids and can be activated via the natural NADPH reductase system. Furthermore, these biocolloids should be amenable to complete acid or enzymic hydrolysis of the DNA to achieve more comprehensive analysis of the DNA adducts if desired. This versatile method should be particularly useful as a chemical complement to established microbiological assays for *in vitro* toxicological screening and enzyme kinetic and inhibition analysis and is particularly well suited for drug discovery and development studies.

#### **ACKNOWLEDGMENT**

This work was supported by US PHS Grant No. ES03154 from the National Institute of Environmental Health Sciences (NIEHS), NIH, U.S.A. The authors thank Marv Thomson for assistance with mass spectrometry.

#### **SUPPORTING INFORMATION AVAILABLE**

Six additional figures showing solution-phase Mb guaiacol product spectra, GC chromatograms for styrene and styrene oxide standards, GC calibrations, chromatograms for SO and HPB generated from cyt P450 2E1 films, HPB calibration curve, and TIC CapLC–MS chromatogram and spectrum obtained for NNK–DNA adducts. This material is available free of charge via the Internet at <http://pubs.acs.org>.

Received for review July 9, 2007. Accepted November 27, 2007.

AC702025F